

Visualization of Water-induced Surface Segregation of Polarons on Rutile TiO₂(110)

Chi M. Yim,^{†,∇} Ji Chen,^{‡,∇} Yu Zhang,[†] Bobbie-Jean Shaw,[†] Chi L. Pang,[†] David C.
Grinter,[†] Hendrik Bluhm,^{§,||} Miquel Salmeron,[⊥] Christopher A. Muryn,[#] Angelos
Michaelides,[‡] and Geoff Thornton^{*,†}

[†] *Department of Chemistry and London Centre for Nanotechnology, University
College London, 20 Gordon Street, London WC1H 0AJ, UK*

[‡] *Department of Physics and Astronomy, London Centre for Nanotechnology and
Thomas Young Centre, University College London, London WC1E 6BT, UK*

[§] *Chemical Sciences Division, Lawrence Berkeley National Laboratory, Berkeley,
California 94720, USA*

^{||} *Advanced Light Source, Lawrence Berkeley National Laboratory, Berkeley,
California 94720, USA*

[⊥] *Materials Science Division, Lawrence Berkeley National Laboratory, Berkeley,
California 94720, USA*

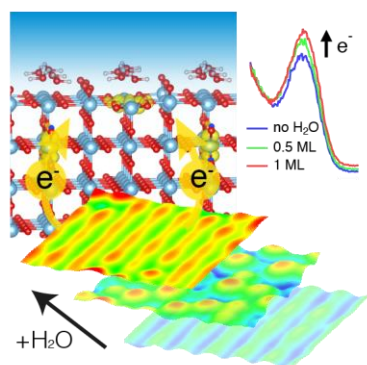
[#] *School of Chemistry, The University of Manchester, Manchester, M13 9PL, UK*

*Corresponding author: g.thornton@ucl.ac.uk

ABSTRACT

Water-oxide surfaces are ubiquitous in nature and of widespread importance to phenomena like corrosion as well as contemporary industrial challenges such as energy production through water splitting. So far a reasonably robust understanding of the structure of such interfaces under certain conditions has been obtained. Considerably less is known about how overlayer water modifies the inherent reactivity of oxide surfaces. Here we address this issue experimentally for rutile $\text{TiO}_2(110)$ using scanning tunneling microscopy and photoemission, with complementary density functional theory calculations. Through detailed studies of adsorbed water nanoclusters and continuous water overlayers, we determine that excess electrons in TiO_2 are attracted to the top surface layer by water molecules. Measurements on methanol show similar behavior. Our results suggest that adsorbate-induced surface segregation of polarons could be a general phenomenon for technologically relevant oxide materials, with consequences for surface chemistry and the associated catalytic activity.

Table of Contents (TOC) Graphic



All real materials contain defects, ranging from atomic vacancies, to interstitials, to impurities, to excess electrons, and more. Defects greatly affect the physical and optical properties of materials and when present at the surfaces of materials can significantly alter the chemical activity of a material. Indeed, a large body of work has shown that defects at the surfaces of materials act as preferential sites for adsorbate binding; sites at which adsorbates are pinned or bonded more strongly and sites with altered catalytic properties.¹⁻³ However, considerably less is known about the other side of this interplay between adsorbates and defects, namely how adsorbates alter the distribution of defects at the surfaces of materials.^{4,5} This is the issue we address in the current study through a detailed set of experiments and simulations of water on rutile TiO₂, in which we focus on the interplay between water and excess electron defects.

The water/rutile TiO₂(110) interface has been selected for this study because of its importance to catalysis and photocatalysis and because it is one of the most widely studied and most well understood of all model oxide surface systems.^{3,6-8} Thanks to this earlier work we now have a broad understanding of the behavior of water on TiO₂(110) at a range of temperatures and water coverages. It is known, for example, that water dissociates at defects on TiO₂(110).⁹⁻¹³ Higher exposure to water at <295 K results in molecular water adsorption at fivefold coordinated Ti (Ti_{5c}) sites, giving rise to the first water layer,¹⁴⁻¹⁶ with some degree of water dissociation.^{17,18} Water monomers and dimers¹⁹ have been observed in scanning tunneling microscopy (STM), along with strand-like features.^{14,20} The latter have been ascribed to continuous hydrogen bonded water chains based on their weak corrugation in STM.²⁰

The behavior of excess electrons on the clean TiO₂(110) surface has also been widely elucidated.²¹⁻²⁷ However, although there has been a theoretical study of

water/anatase interfaces,⁴ the impact of water on the excess electrons on rutile remains poorly understood. Here we probe the first layer of adsorbed water on rutile TiO₂(110) with STM, photoemission, and density functional theory (DFT). We find that adsorbed water molecules draw electrons from within TiO₂ to the surface. This electronic coupling is also evidenced in photoemission under near ambient conditions, with a similar behavior observed for methanol.

We start by discussing our measurements of various water structures on TiO₂(110) performed in the filled states imaging mode in STM, which draw attention to the interaction of water molecules with excess electrons on the surface. More conventional empty-states images are also provided for comparison. When imaging TiO₂(110) in filled states STM (with the sample bias set at -1 V), electrons are sampled from the Fermi level (E_F) to the band-gap states (BGS) peak (located at 1 eV below E_F) of the TiO₂ sample. As a consequence, in addition to the bright Ti-dark O row contrast that is usually seen in the empty- states image (inset of Figure 1a), the filled states image also exhibits lobe-like features along the Ti_{5c} rows (inset of Figure 1b). The lobe-like features correspond to the BGS electrons (or excess electrons) in TiO₂ (110) created as a result of O_b-vac formation (marked by black dots in the insets of Figure 1, a and b).^{21,22,28}

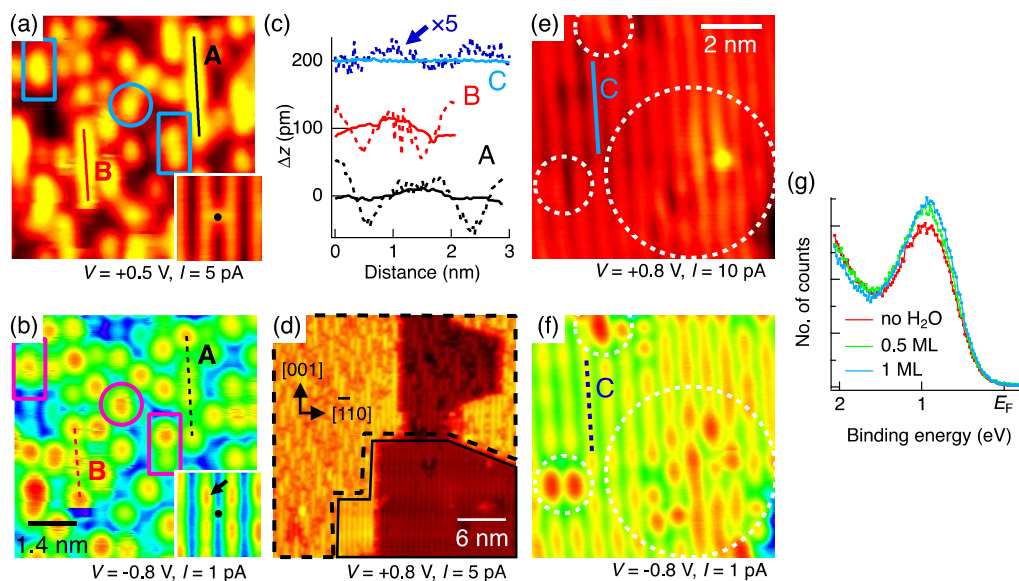


Figure 1. Small water clusters, *nanostructured* and *continuous* water chains on rutile $\text{TiO}_2(110)$. (a-b) Simultaneously recorded (a) empty- and (b) filled- states (*dual-mode*) STM images of *r*- $\text{TiO}_2(110)$, recorded after exposure to 0.65 L H_2O at 78 K. Circles and rectangles mark water monomers and dimers (or trimers) on the Ti_{5c} rows, respectively. Insets of (a-b): *Dual-mode* images recorded in the vicinity of an $\text{O}_b\text{-vac}$ (marked by a black dot) on *r*- TiO_2 . An arrow indicates one of the lobe-like features on the Ti_{5c} rows. (c) Line profiles taken along two strands in (a-b), and that taken along one section of the *continuous* water chain in (e-f). Solid (dashed) lines correspond to line profiles taken from the empty- (filled-) states images in (a,e) [(b,f)] (d) Empty states STM image taken from the surface in (a) after annealing to 146 K. The imaged area consists of both the *disordered* and *perfect* regions (see definitions in the main text). (e-f) *Dual-mode* STM images of the *perfect* region. Circles mark subsurface charge impurities. STM images in (a-b) were taken at 78 K, those in (d-f) at 146 K. (g) He I ($h\nu = 21.2$ eV) band-gap state (BGS) region UPS spectra of the as-prepared $\text{TiO}_2(110)$ surface (red), and that with 0.5 (green) and 1 ML (blue) H_2O . All spectra were recorded at a grazing emission angle of 15° from the surface [001] azimuth, at ~ 200 K. All the UPS spectra presented are raw data. Error bars are represented by the scatter in the data points. See Figure S10 for the corresponding He II ($h\nu = 40.8$ eV) spectra.

Exposing a $\text{TiO}_2(110)$ surface that has been reduced to form oxygen vacancies [*r*- $\text{TiO}_2(110)$] to 0.65 L Langmuirs ($1 \text{ L} = 1.33 \times 10^{-6} \text{ mbar.s}$) of water at 78 K leads to a number of water structures on the Ti_{5c} rows (Figure 1a). These include water monomers (marked with circles), dimers (or trimers) (marked with rectangles),¹⁹ and

strand-like features (or strands).^{14,20} Based on the very weak corrugation measured along the strands in the empty-states STM, Lee *et al.*²⁰ proposed that they are *continuous* water chains, i.e. with water molecules adsorbed on every Ti_{5c} site along the row. Instead, our STM data reveal that they are not *continuous* water chains: in the filled states STM (Figure 1b), each strand is further resolved into a number of protrusions, giving an overall corrugation of ~80 pm along the strands (Figure 1c). Contrary to previous work, we propose that the strands shown in Figure 1, a and b are *nanostructured* chains, consisting of discrete water monomers and dimers (and/or trimers) separated by at least two lattice spacings along the [001].

To substantiate the suggestion that the strands observed at 78 K are not *continuous*, we attempted to form *continuous* water chains by heating the surface to 146 K [see SI, Section S3 additional details]. The imaged area now consists of two different regions (Figure 1d). One region, enclosed with a dashed outline, consists of water monomers, dimers (or trimers) and strands that we refer to as the *disordered* region. Another region, enclosed with a solid outline, consists of nearly perfect rows running along the [001] direction, which we refer to as the *perfect* region. Line profile taken across both regions (Figure S1) indicates that both the rows in the *perfect* region and strands in the *disordered* region have the same height.

Our high-resolution STM images (Figure 1, e and f) provide evidence that the rows in the *perfect* region have different internal structure as compared to the strands. Unlike the strands that are further resolved into separate protrusions in the filled states STM (Figure 1b), the bright rows in the *perfect* region have very weak corrugation along the row direction (Figure 1f). Note that some parts of the *perfect* region (marked in dashed circles) exhibit significantly increased corrugation in both empty- and filled- states STM, which we attribute to Ti³⁺ interstitials that lie in the sub-

surface region of $\text{TiO}_2(110)$.²⁹ On this basis, we assign the rows in the *perfect* region to *continuous* water chains. As these chains are formed on each Ti_{5c} row, a complete monolayer (ML) of water film is formed where 1 ML corresponds to the number of Ti_{5c} sites.

Owing to their closely-packed nature, we do not expect the water molecules within a *continuous* water chain to exhibit any noticeable contrast along the row direction, even in the filled-states image. Nevertheless, a small corrugation is observed in the dashed line profile of C in Figure 1f, as well as in the rows to left of line C. We ascribe this to coupling with electron polarons that are attracted to the surface by the water molecules. The band gap states (BGS) that are sampled in the filled-states images are polaronic in origin and hence form the contrast in the image.^{21,22,28}

To test these ideas we performed DFT calculations on clean and water-covered surfaces containing an O_b -vac. In the SI, Section S4 we show the continuous water chain indeed has slightly preferred adsorption energy, whereas nanostructured water chain is likely to form due to kinetics. With these in mind, we now discuss the impact of water on surface polarons when *continuous* water chains are adsorbed on all the Ti_{5c} rows. Because defects are involved, for these calculations we employed a Hubbard U correction³⁰ (specifically PBE+U) as well as the hybrid Heyd-Scuseria-Ernzerhof (HSE) functional.³¹ The creation of an O_b -vac leads to two excess electrons in the slab. To establish where these electrons reside at both the clean and water covered surfaces we generated an ensemble of 20 surface models in which the Ti atoms in the first and second surface layer were randomly displaced from their optimal positions in the defect-free slab. These structures were subsequently geometry optimized and the location of the excess electrons examined. We find that for the

clean surface the excess electrons mostly appear in the second layer (67%), which agrees with previous studies.^{21,22,28,32} In the case of the water-covered surface, however, the excess electrons are mostly located in the topmost layer (75%). Three typical configurations for the excess electrons at the water-covered surface are shown in Figure 2, a to c. In the ‘Surf-1’ configuration, one excess electron is localized in the first surface layer while the other is delocalized. In the ‘Mixed-1’ configuration, one electron is located in the first layer and another in the second layer. In the ‘Sub-1’ configuration both are in the second layer. Other configurations considered for the water film are shown in Figure S6.

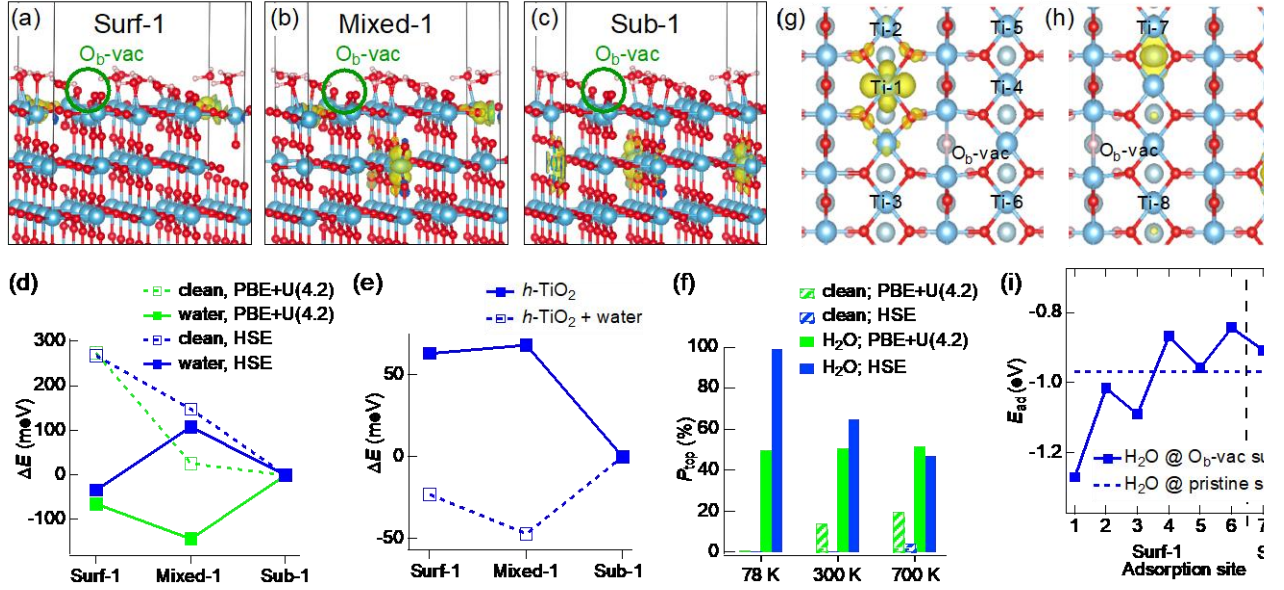


Figure 2. Stability of different excess electron configurations. (a-c) Three different locations of excess electrons induced by O_b -vac on the $TiO_2(110)$ surface with 1 ML of H_2O : (a) first layer (Surf-1); (b), first and second layer (Mixed-1); (c) second layer (Sub-1). (d) Total energy difference between Surf-1, Mixed-1 and Sub-1 with and without water calculated using different methods plotted with Sub-1 as the reference. (e) Energies of Surf-1, Mixed-1 and Sub-1 configurations calculated on a hydroxylated surface model using PBE+U ($U=4.2$ eV). (f) Percentage of polarons in the topmost surface layer estimated according to a Boltzmann distribution, $P(E) \propto \exp\left(-\frac{E}{kT}\right)$, where k is Plank's constant, T is temperature, and E is the total energy of each polaron configuration. (g) Surf-1 and (h) Sub-1 configurations for excess electrons. The Ti sites labeled have been considered for the adsorption of single water and methanol molecules. (i) Adsorption energy (E_{ad}) of a single water molecule at sites of different Surf-1 and Sub-1 configurations. These results are based on a (4×2) supercell with 4 trilayers. A single O_b -vac is introduced in the supercells as indicated in (a-c).

Figure 2d shows the energy difference between the ‘Surf-1’, ‘Mixed-1’ and ‘Sub-1’ configurations with and without water, calculated using the two different exchange-correlation functionals. The ‘Surf-1’ configuration is much less stable without water and becomes more stable when the water film covers the surface, indicating a strong water-polaron interaction that attracts the excess electrons towards the top surface layer. For the ‘Mixed-1’ structure, as it contains both first layer and second layer excess electrons, we see a strong dependence of the relative energy on

the computational approach used (specifically the exchange-correlation functional). However, we show below that if we consider all configurations together, the results in terms of the location of the excess electron are less sensitive to the functional used (also see Figure S7).

Figure 2e shows the energy difference between the three configurations ('Surf-1', 'Mixed-1' and 'Sub-1') with and without water, calculated on a hydroxylated surface model [h -TiO₂(110), Figure S8], using PBE+ U with U set at 4.2 eV. As shown in Figure 2f, without water the polaronic state 'Sub-1' is most stable. With water, polaronic states 'Surf-1' and 'Mixed-1' are more stable. We also note that without water, polaronic state 'Surf-1' of the h -TiO₂(110) model readily transforms to the 'Mixed-1' state after optimization, showing that the 'Surf-1' state is unstable without water. Hence, these calculations demonstrate that water stabilizes surface polarons also on h -TiO₂(110).

Assuming the population of sites for the excess electron follows a Boltzmann distribution, the proportion of excess electrons in the first layer as a function of temperature has been estimated. As reported in Figure 2f, this shows a large increase upon going from the clean surface to the water-covered surface. In the SI, we show that our results remain valid with the inclusion of more excess electron configurations and for a thicker TiO₂ slab (Figures S7 and S9). Our estimate for the clean surface also agrees qualitatively with previous molecular dynamics sampling at high temperatures.^{22,32} Our estimate of the polaron distribution is based on a description of the full potential energy surface with a limited number of representative configurations. *Ab initio* molecular dynamics simulations with advanced sampling techniques are desirable to further shed light on how water impacts the finite temperature dynamics of polarons.

We have also calculated the interaction of a water monomer on different sites of the ‘Surf-1’ and ‘Sub-1’ configurations (Figure 2, g and h). In Figure 2i we plot these adsorption energies together with those on a defect free surface. We see that when the H₂O is adsorbed on the same row as the excess charge, there is a significant attractive interaction. In particular, when the H₂O molecule sits directly above the excess electron, the interaction can be as large as 0.3 eV. The Ti_{5c}-OH₂ bond length, however, shows a small contraction from 2.206 to 2.202 Å upon adding an excess electron, suggesting that the total interaction increase is largely due to the stabilization of the polaron by water instead of the enhanced adsorption of water alone. Similar water-polaron coupling has recently been predicted for water at an anatase surface, where the results indicate that it should trigger water dissociation.⁴

Ultraviolet photoelectron spectroscopy (UPS) experiments provide further evidence for the enrichment of excess electrons at the surface upon water adsorption. The measurements were performed at a grazing emission angle of 15° from the [001] azimuth. Under these conditions the sampling depth is only one-fourth of that in normal emission, leading to enhanced surface sensitivity.

Our UPS spectra in Figure 1g evidence a clear increase of the BGS peak after dosing 1 ML water on TiO₂(110) at 200 K. There is a corresponding decrease in the work function by about 0.8 eV that changes the kinetic energy of photoelectrons. This might have a minor effect on the spectral intensity, which should be eliminated by spectra normalization. An increase in the BGS peak intensity on exposure to H₂O was also observed at 300 K in early work using a cylindrical mirror analyser,³³ which has an acceptance angle of 42±6°. Such an increase has not been reported for previous UPS measurements involving low temperature H₂O exposure. We ascribe this to the normal emission geometry used in those studies, giving rise to a lower surface

sensitivity.³⁴ The increase in BGS peak intensity therefore indicates that a greater quantity of excess electrons is located at the surface/subsurface regime when H₂O is adsorbed.

So far we have found that water promotes the segregation of electrons to the TiO₂(110) surface under UHV conditions. To explore if similar behavior can be observed in a more practical environment of photochemistry, we performed a series of ambient pressure photoemission (APPEs) measurements. Figure 3 shows APPEs data recorded following exposure of hydroxylated TiO₂(110) (*h*-TiO₂) to water vapor up to a partial pressure (P_{water}) of 0.53 mbar. An increase up to 1.3×10^{-4} mbar leads to an increase in the OH density, as indicated by the increase in the peaks corresponding to the hydroxyl σ and π molecular orbitals (Figure 3b). Dosing H₂O at such relatively high pressures exposes the sample to a non-negligible partial pressure of O₂ resulting from residual gas dissolved in the liquid water, an effect that is unavoidable based on the current technical limits for high pressure measurements. It is known from previous work that the resulting oxidation reaction leads to the formation of terminal OH groups, which saturates at 0.5 ML.³⁵ The presence of this reaction explains both the increase in OH density and the decrease in the BGS peak (Figure 3c).

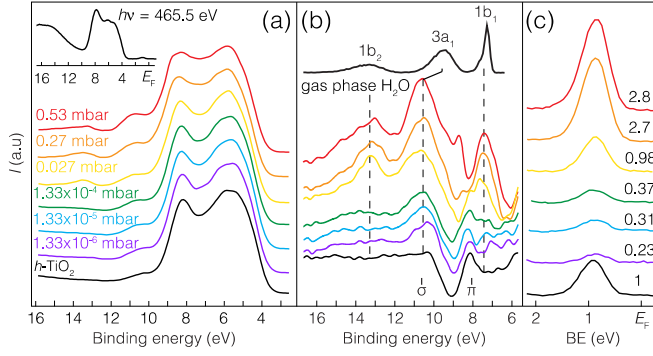


Figure 3. APPES measurements on water/TiO₂(110) at increasing water vapor pressure (P_{water}). (a) Valence band spectra ($h\nu = 455$ eV) acquired at incremental P_{water} . Inset shows a valence band spectrum of the hydroxylated TiO₂ surface recorded at the L₃ resonance energy ($h\nu = 465.5$ eV) (b) Corresponding difference spectra of those in (a), obtained by subtracting each spectrum from that of a clean, OH-free surface (recorded from the as-prepared surface kept at ~ 575 K, not shown). In (b), the spectrum in black is of H₂O in the gas-phase, obtained by retracting the sample by 2.1 mm, aligned at the 1b₁ molecular orbital of the difference spectra. The positions of the σ and π hydroxyl molecular orbitals are indicated. All the spectra are vertically shifted for clarity. (c) Corresponding resonant photoemission spectra ($h\nu = 465.5$ eV) of the BGS peak recorded at increasing P_{water} . The number above each spectrum represents the normalized intensity of the BGS peak relative to that of h -TiO₂. All the spectra in (a-c) are presented using the same color code.

Further increasing P_{water} to near ambient conditions leads to other changes in the spectra. As P_{water} reaches 2.7×10^{-2} mbar, the OH features do not increase further. Instead, an additional set of peaks, which correspond to 1b₂, 3a₁ and 1b₁ molecular orbitals of water (Figure 3b),¹⁴ start to emerge, and increase in intensity with P_{water} up to its maximum value at 0.53 mbar (equivalent to a H₂O coverage of ~ 2.7 ML). Hydroxylation followed by molecular water adsorption was also found in an earlier APPES study.³⁶ The corresponding increase of the BGS peak in the resonant photoemission spectra (Figure 3c) is attributed to the migration of electron polarons from deep-lying Ti interstitials attracted by water at the interface, which is reversible after removing the water (see Figure S11). This degree of enhancement is also observed off-resonance (not shown). Molecular dynamics simulations for liquid water

on $\text{TiO}_2(110)$ with 0.5 ML terminal OH indicate that the time averaged coverage of molecular water on bare Ti_{5c} sites is 0.18 ML.³⁵ These results indicate that the adsorbate-induced charge segregation to the surface of TiO_2 also occurs in the ambient pressure range relevant to practical applications. The larger enhancement observed compared with that in Fig. 1g presumably arises because of the temperature of the substrate, with an increased mobility of electron polarons at 260 K compared with 200 K.

In addition, we have performed additional STM and UPS measurements on *r*- TiO_2 using methanol as a probe to show the charge-segregation on polaronic surfaces is not limited to water, but a rather general phenomenon. Our results are summarized in Figure 4. At low coverage (Figure 4a), single methanol molecules are adsorbed at the Ti_{5c} sites (see model in Figure 4f). When two methanol molecules adsorb at adjacent Ti_{5c} sites, they form a HB with each other, becoming a dimer.³⁷ Similar to water, methanol also appear as protrusions in the filled-states image (Figure 4b). As coverage increases, short chains composed of two dimers, as well as continuous chains of methanol molecules are also formed (Figure S13). At a saturation coverage of 0.67 ML (Figure 4c), methanol forms an ordered structure with a $L(1\times 3)$ unit cell.³⁷ As shown by photoemission (Figure 4d), methanol adsorption on $\text{TiO}_2(110)$ also leads to an increase in the BGS peak intensity. This is corroborated by the results of the calculations (Figure 4e), showing that methanol, when adsorbed on *r*- TiO_2 , also prefers a configuration with excess electrons in the topmost surface layer (i.e. ‘Surf-1’, see Figure 2).

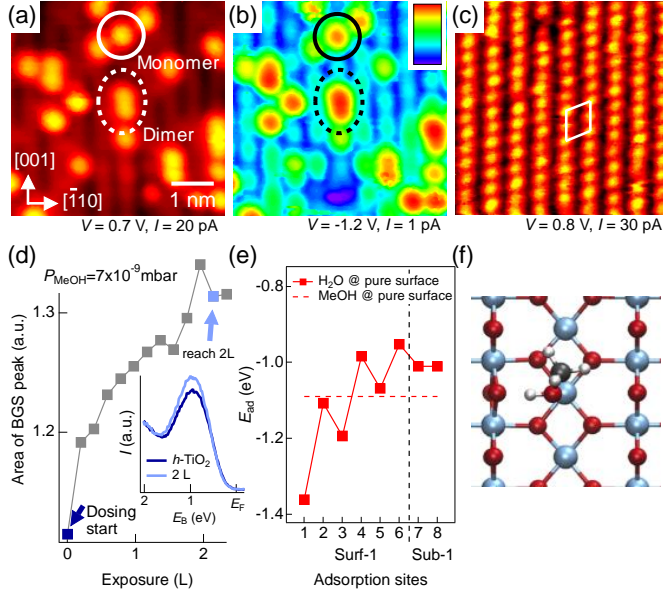


Figure 4. Methanol adsorption affects excess electron distribution in TiO₂. (a-b) 6 × 6 nm² Simultaneously recorded (a) empty- and (b) filled- states STM images of the reduced TiO₂(110) surface recorded after a methanol exposure of 0.04 L. Solid (dashed) lines mark methanol monomer (dimer) species. (c) 6 × 6 nm² empty-states image of the same surface covered with 0.67 ML of methanol. A rhombus marks the L(1 × 3) unit cell formed by methanol molecules. All STM images were recorded at 78 K. (d) Plot of BGS peak area versus methanol exposure. The data set was obtained by collecting He I ($h\nu = 21.2$ eV) photoemission spectra near the BGS region (~ 1 eV below E_F) while the as-prepared, h -TiO₂ surface was continuously exposed to 7×10^{-9} mbar of methanol at a sample temperature of ~ 200 K. The inset shows two of the spectra, taken at the start (light blue) and when methanol exposure reaches 2 L (dark blue), respectively. (e) Adsorption energies (E_{ad}) of single methanol molecules at different sites on the reduced TiO₂(110) surfaces (O_b -vac) with ‘Surf-1’ and ‘Sub-1’ configurations for excess electrons (see Figure 2 for details). Dashed lines are their E_{ad} on the stoichiometric surface. (f) Ball and stick model of the lowest energy configuration of a single methanol molecule adsorbed at a Ti_{5c} site.

In conclusion, this study has shown that low temperature adsorption of water on TiO₂(110) results in discrete molecules and dimers rather than *continuous* chains. Our DFT calculations indicate that *continuous* chains are thermodynamically stable, but kinetic barriers associated with hydrogen bond rearrangement limit their formation. Crucially, our experiments and calculations also indicate that excess electrons in TiO₂ are attracted to the top surface layer by water as a result of strong-

adsorbate-polaron coupling. A similar behavior is observed for methanol, suggesting that it is a general phenomenon. Our photoemission measurements reveal that such interactions between electron polarons in the substrate and adsorbates also occur at near ambient conditions.

The adsorbate-induced attraction of electrons to the surfaces of materials could have significant consequences for their physiochemical properties. It may cause the trapping, relaxation and recombination of photo-excited carriers, as well as band bending near the surface. Moreover, knowledge of the molecule-induced surface affinity to electron polarons may help to find specific molecule combinations leading to the control of catalytic properties of polaronic materials. Finally, enhanced segregation of electrons, beyond the levels observed here for TiO₂, could even destabilize the surface itself leading to surface reconstruction or dissolution.

ASSOCIATED CONTENT

Supporting Information The Supporting Information is available free of charge on the ACS Publications website at D.O.I:...

Experimental details, computational details, supporting sections, and Figure S1-S13 (PDF).

AUTHOR INFORMATION

Corresponding Author: *G.T.: E-mail: g.thornton@ucl.ac.uk

Author Contributions: [∇]C.M.Y. and J.C. contributed equally to this work.

Notes: The authors declare no competing financial interest.

ACKNOWLEDGEMENTS

C.M.Y., Y.Z., C.P. and G.T are supported by the European Research Council Advanced Grant ENERGYSURF (G.T.), European Cooperation in Science and Technology Action CM1104, and the Alexander von Humboldt Stiftung (Germany). J.C. and A.M. are supported by the European Research Council under the European Union's Seventh Framework Programme (FP/2007-2013) / ERC Grant Agreement number 616121 (HeteroIce project). We also grateful for computational resources to the UKCP consortium through EPSRC grant (EP/F036884/1), London Centre for Nanotechnology and UCL research computing. G.T. and A.M. are also supported by the Royal Society through Royal Society Wolfson Research Merit Awards. HB and MS acknowledge support by the Director, Office of Science, Office of Basic Energy Sciences, and by the Division of Chemical Sciences, Geosciences and Biosciences (HB) and Materials Sciences (MS) of the U.S. Department of Energy at LBNL under Contract No. DE-AC02-05CH11231.

References

- (1) *Defects at Oxide Surfaces, Springer Series in Surface Sciences*; Jupille, J., Thornton, G., Eds.; Springer International Publishing: Cham, 2015; Vol. 58.
- (2) Haruta, M.; Tsubota, S.; Kobayashi, T.; Kageyama, H.; Genet, M. J.; Delmon, B. Low-Temperature Oxidation of CO Over Gold Supported on TiO₂, α -Fe₂O₃, and Co₃O₄. *J. Catal.* **1993**, *144*, 175–192.
- (3) Saavedra, J.; Doan, H. A.; Pursell, C. J.; Grabow, L. C.; Chandler, B. D. The Critical Role of Water at the Gold-Titania Interface in Catalytic CO Oxidation. *Science* **2014**, *345*, 1599–1602.
- (4) Selcuk, S.; Selloni, A. Facet-Dependent Trapping and Dynamics of Excess Electrons at Anatase TiO₂ Surfaces and Aqueous Interfaces. *Nat. Mater.* **2016**, *15*, 1107–1112.
- (5) Cao, Y.; Yu, M.; Qi, S.; Huang, S.; Wang, T.; Xu, M.; Hu, S.; Yan, S. Scenarios of Polaron-Involved Molecular Adsorption on Reduced TiO₂(110) Surfaces. *Sci. Rep.* **2017**, *7*, 6148.
- (6) Pang, C. L.; Lindsay, R.; Thornton, G. Structure of Clean and Adsorbate-Covered Single-Crystal Rutile TiO₂ Surfaces. *Chem. Rev.* **2013**, *113*, 3887–3948.
- (7) Björneholm, O.; Hansen, M. H.; Hodgson, A.; Liu, L.-M.; Limmer, D. T.; Michaelides, A.; Pedevilla, P.; Rossmeisl, J.; Shen, H.; Tocci, G.; et al. Water at Interfaces. *Chem. Rev.* **2016**, *116*, 7698–7726.
- (8) Mu, R.; Zhao, Z.-J.; Dohnálek, Z.; Gong, J. Structural Motifs of Water on Metal Oxide Surfaces. *Chem. Soc. Rev.* **2017**, *46*, 1785–1806.
- (9) Wendt, S.; Matthiesen, J.; Schaub, R.; Vestergaard, E. K.; Lægsgaard, E.; Besenbacher, F.; Hammer, B. Formation and Splitting of Paired Hydroxyl Groups on Reduced TiO₂(110). *Phys. Rev. Lett.* **2006**, *96*, 066107.
- (10) Henderson, M. A.; Epling, W. S.; Peden, C. H. F.; Perkins, C. L. Insights Into Photoexcited Electron Scavenging Processes on TiO₂ Obtained From Studies of the Reaction of O₂ With OH Groups Adsorbed at Electronic Defects on TiO₂(110). *J. Phys. Chem. B* **2003**, *107*, 534–545.
- (11) Bikondoa, O.; Pang, C. L.; Ithnin, R.; Muryn, C. A.; Onishi, H.; Thornton, G. Direct Visualization of Defect-Mediated Dissociation of Water on TiO₂(110). *Nat. Mater.* **2006**, *5*, 189–192.
- (12) Zhang, Z.; Bondarchuk, O.; Kay, B. D.; White, J. M.; Dohnalek, Z. Imaging Water Dissociation on TiO₂(110): Evidence for Inequivalent Geminate OH Groups. *J. Phys. Chem. B* **2006**, *110*, 21840–21845.
- (13) Petrik, N. G.; Kimmel, G. A. Reaction Kinetics of Water Molecules with Oxygen Vacancies on Rutile TiO₂(110). *J. Phys. Chem. C* **2015**, *119*, 23059–23067.
- (14) Brookes, I. M.; Muryn, C. A.; Thornton, G. Imaging Water Dissociation on TiO₂(110). *Phys. Rev. Lett.* **2001**, *87*, 266103.
- (15) Liu, L.-M.; Zhang, C.; Thornton, G.; Michaelides, A. Structure and Dynamics of Liquid Water on Rutile TiO₂(110). *Phys. Rev. B* **2010**, *82*, 161415.
- (16) Kimmel, G. A.; Baer, M.; Petrik, N. G.; VandeVondele, J.; Rousseau, R.; Mundy, C. J. Polarization- and Azimuth-Resolved Infrared Spectroscopy of Water on TiO₂(110): Anisotropy and the Hydrogen-Bonding Network. *J. Phys. Chem. Lett.* **2012**, *3*, 778–784.
- (17) Allegretti, F.; O'Brien, S.; Polcik, M.; Sayago, D. I.; Woodruff, D. P.

- Adsorption Bond Length for H₂O on TiO₂(110): A Key Parameter for Theoretical Understanding. *Phys. Rev. Lett.* **2005**, *95*, 226104.
- (18) Amft, M.; Walle, L. E.; Ragazzon, D.; Borg, A.; Uvdal, P.; Skorodumova, N. V.; Sandell, A. A Molecular Mechanism for the Water–Hydroxyl Balance During Wetting of TiO₂. *J. Phys. Chem. C* **2013**, *117*, 17078–17083.
- (19) Matthiesen, J.; Hansen, J. Ø.; Wendt, S.; Lira, E.; Schaub, R.; Lægsgaard, E.; Besenbacher, F.; Hammer, B. Formation and Diffusion of Water Dimers on Rutile TiO₂(110). *Phys. Rev. Lett.* **2009**, *102*, 226101.
- (20) Lee, J.; Sorescu, D. C.; Deng, X.; Jordan, K. D. Water Chain Formation on TiO₂(110). *J. Phys. Chem. Lett.* **2013**, *4*, 53–57.
- (21) Yim, C. M.; Watkins, M. B.; Wolf, M. J.; Pang, C. L.; Hermansson, K.; Thornton, G. Engineering Polarons at a Metal Oxide Surface. *Phys. Rev. Lett.* **2016**, *117*, 116402.
- (22) Setvin, M.; Franchini, C.; Hao, X.; Schmid, M.; Janotti, A.; Kaltak, M.; Van de Walle, C. G.; Kresse, G.; Diebold, U. Direct View at Excess Electrons in TiO₂ Rutile and Anatase. *Phys. Rev. Lett.* **2014**, *113*, 086402.
- (23) Sezen, H.; Buchholz, M.; Nefedov, A.; Natzeck, C.; Heissler, S.; Di Valentin, C.; Wöll, C. Probing Electrons in TiO₂ Polaronic Trap States by IR-Absorption: Evidence for the Existence of Hydrogenic States. *Sci. Rep.* **2014**, *4*, 53.
- (24) Moser, S.; Moreschini, L.; Jaćimović, J.; Barišić, O. S.; Berger, H.; Magrez, A.; Chang, Y. J.; Kim, K. S.; Bostwick, A.; Rotenberg, E.; et al. Tunable Polaronic Conduction in Anatase TiO₂. *Phys. Rev. Lett.* **2013**, *110*, 196403.
- (25) Deskins, N. A.; Rousseau, R.; Dupuis, M. Defining the Role of Excess Electrons in the Surface Chemistry of TiO₂. *J. Phys. Chem. C* **2010**, *114*, 5891–5897.
- (26) Deskins, N. A.; Rousseau, R.; Dupuis, M. Distribution of Ti³⁺ Surface Sites in Reduced TiO₂. *J. Phys. Chem. C* **2011**, *115*, 7562–7572.
- (27) Deskins, N. A.; Rousseau, R.; Dupuis, M. Correction to “Localized Electronic States From Surface Hydroxyls and Polarons in TiO₂(110),” “Defining the Role of Excess Electrons in the Surface Chemistry of TiO₂,” And “Distribution of Ti³⁺ Surface Sites in Reduced TiO₂.” *J. Phys. Chem. C* **2014**, *118*, 13326–13327.
- (28) Papageorgiou, A. C.; Beglitis, N. S.; Pang, C. L.; Teobaldi, G.; Cabailh, G.; Chen, Q.; Fisher, A. J.; Hofer, W. A.; Thornton, G. Electron Traps and Their Effect on the Surface Chemistry of TiO₂(110). *Proc. Natl. Acad. Sci. U.S.A.* **2010**, *107*, 2391–2396.
- (29) Yoon, Y.; Du, Y.; Garcia, J. C.; Zhu, Z.; Wang, Z.-T.; Petrik, N. G.; Kimmel, G. A.; Dohnálek, Z.; Henderson, M. A.; Rousseau, R.; et al. Anticorrelation Between Surface and Subsurface Point Defects and the Impact on the Redox Chemistry of TiO₂(110). *ChemPhysChem* **2014**, *16*, 313–321.
- (30) Dudarev, S. L.; Botton, G. A.; Savrasov, S. Y.; Humphreys, C. J.; Sutton, A. P. Electron-Energy-Loss Spectra and the Structural Stability of Nickel Oxide: an LSDA+U Study. *Phys. Rev. B* **1998**, *57*, 1505–1509.
- (31) Heyd, J.; Scuseria, G. E.; Ernzerhof, M. Erratum: “Hybrid Functionals Based on a Screened Coulomb Potential” [J. Chem. Phys. 118, 8207 (2003)]. *J. Chem. Phys.* **2006**, *124*, 219906.
- (32) Kowalski, P. M.; Camellone, M. F.; Nair, N. N.; Meyer, B.; Marx, D. Charge Localization Dynamics Induced by Oxygen Vacancies on the TiO₂(110)

- Surface. *Phys. Rev. Lett.* **2010**, *105*, 146405.
- (33) Kurtz, R. L.; Stock-Bauer, R.; Madey, T. E.; Román, E.; De Segovia, J. L. Synchrotron Radiation Studies of H₂O Adsorption on TiO₂(110). *Surf. Sci.* **1989**, *218*, 178–200.
- (34) Payne, D. T.; Zhang, Y.; Pang, C. L.; Fielding, H. H.; Thornton, G. Coverage-Dependent Two-Photon Photoexcitation at the H₂O/TiO₂ Interface. *Surf. Sci.* **2016**, *652*, 189–194.
- (35) Hussain, H.; Tocci, G.; Woolcot, T.; Torrelles, X.; Pang, C. L.; Humphrey, D. S.; Yim, C. M.; Grinter, D. C.; Cabailh, G.; Bikondoa, O.; et al. Structure of a Model TiO₂ Photocatalytic Interface. *Nat. Mater.* **2017**, *16*, 461–466.
- (36) Ketteler, G.; Ogletree, D. F.; Bluhm, H.; Liu, H.; Hebenstreit, E. L. D.; Salmeron, M. In Situ Spectroscopic Study of the Oxidation and Reduction of Pd(111). *J. Am. Chem. Soc.* **2005**, *127*, 18269–18273.
- (37) Silber, D.; Kowalski, P. M.; Traeger, F.; Buchholz, M.; Bebensee, F.; Meyer, B.; Wöll, C. Adsorbate-Induced Lifting of Substrate Relaxation Is a General Mechanism Governing Titania Surface Chemistry. *Nat. Commun.* **2016**, *7*, 12888.